

Crystal structure and magnetic properties of the spinel compound $\text{Fe}_{0.76}\text{In}_{2.17}\text{S}_4$

Alexander Krimmel, Z. Seidov, G. G. Guseinov, A. I. Najafov, Hans-Albrecht Krug von Nidda, Alois Loidl, D. M. Többens

Angaben zur Veröffentlichung / Publication details:

Krimmel, Alexander, Z. Seidov, G. G. Guseinov, A. I. Najafov, Hans-Albrecht Krug von Nidda, Alois Loidl, and D. M. Többens. 2005. "Crystal structure and magnetic properties of the spinel compound $\text{Fe}_{0.76}\text{In}_{2.17}\text{S}_4$." *Journal of Physics: Condensed Matter* 17 (23): 3611–18.
<https://doi.org/10.1088/0953-8984/17/23/013>.

Crystal structure and magnetic properties of the spinel compound $\text{Fe}_{0.76}\text{In}_{2.17}\text{S}_4$

A Krimmel¹, Z Seidov^{1,2}, G G Guseinov², A I Najafov³,
H-A Krug von Nidda¹, A Loidl¹ and D M Többens^{4,5}

¹ Experimentalphysik V, Elektronische Korrelationen und Magnetismus, Universität Augsburg, D-86159 Augsburg, Germany

² Institute of Physics, Azerbaijan National Academy of Science, AZ-1143 Baku, Azerbaijan

³ Institute of Radiation Problems, Azerbaijan National Academy of Science, H Javid Street 31a, AZ-1143 Baku, Azerbaijan

⁴ Hahn-Meitner-Institut, D-14109 Berlin, Germany

Abstract

In the search for new materials exhibiting both ferromagnetic and semiconducting properties, approximately 10% Fe has been incorporated into the large gap semiconductor In_2S_3 , resulting in a new spinel compound $\text{Fe}_{0.76}\text{In}_{2.17}\text{S}_4$. Magnetic measurements show properties of a canonical spin glass state below a freezing temperature of $T_F = 5$ K. Standard powder x-ray diffraction at room temperature revealed the cubic spinel structure. Further structural investigations by high-resolution neutron powder diffraction in the temperature range $1.6 \text{ K} \leq T \leq 280 \text{ K}$ confirmed the spinel structure with an almost complete cation inversion corresponding to an inversion parameter of 0.94. A mutually consistent description of the neutron diffraction data, EDX analysis and magnetic measurements show that the present compound may be written as $(\text{Fe}_{0.04}\text{In}_{0.89}\square_{0.07})^A(\text{Fe}_{0.72}\text{In}_{1.28})^B\text{S}_4$, with \square denoting vacancies. No magnetic intensities could be observed, in agreement with a spin glass state.

(Some figures in this article are in colour only in the electronic version)

1. Introduction

Ferromagnetic semiconductors are materials that simultaneously exhibit semiconducting properties and spontaneous long-range ferromagnetic order. Classic examples include europium chalcogenides and chalcogenide spinels. The discovery of ferromagnetic order in $\text{In}_{1-x}\text{Mn}_x\text{As}$ [1] and in $\text{Ga}_{1-x}\text{Mn}_x\text{As}$ [2] has triggered an enormous research effort, as ferromagnetic properties have been detected in materials already widely used in semiconducting device applications. Currently, there is a global race to develop ferromagnetic

⁵ Present address: Institut für Mineralogie und Petrographie, Universität Innsbruck, A-6020 Innsbruck, Austria.

semiconducting materials with a Curie temperature T_C reaching room temperature (or exceeding it). Ferromagnetic semiconductors will allow the development of new devices in spintronics with electronic and optical signal processing, as well as magnetic memory functionality.

β - In_2S_3 is a large gap semiconductor, and it has recently attracted great interest as a window material in thin-film photovoltaic devices in order to replace CdS for environmental reasons [3]. Furthermore, the optical band gap can be tuned by varying the material preparation conditions appropriately [4].

At ambient pressure, the spinel compound In_2S_3 exists in three different phases, labelled α , β and γ , respectively. Usually, spinels exhibit the stoichiometry AB_2X_4 with tetrahedrally coordinated A-sites at the Wyckoff position (8a) (1/8, 1/8, 1/8), octahedrally coordinated B-sites at the Wyckoff position 16d (1/2, 1/2, 1/2), and chalcogenide ions at the X-site (32e) (x, x, x) with $x = 0.25$ for the ideal spinel structure, respectively. The cation distribution of In_2S_3 may be written as $(\text{In}_{0.67}^{\text{A}}\square_{0.33})\text{In}_2^{\text{B}}\text{S}_4$, with \square denoting unoccupied A-sites. For an ordered distribution of cations and vacancies at the tetrahedral site the β -phase is formed, and for a disordered distribution the α -phase is formed [5]. The β -phase of In_2S_3 is stable from low temperatures up to 693 K and forms a tetragonal variant of the spinel structure [6, 7]. The structure of β - In_2S_3 can be described by space group $I4_1/amd$ with room-temperature lattice constants of $a \approx 7.61$ Å and $c \approx 32.31$ Å. Indium ions are located at a tetrahedral site corresponding to the Wyckoff position (8e), one octahedral site at (8c) and a second octahedral site at (16h). Sulfur is distributed over three inequivalent (16h) sites [6, 7]. All sites are fully occupied.

On increasing the metal content slightly to $\text{In}_{2.77}\text{S}_4$, the normal cubic spinel structure is found with In ions at the A-site occupied to 77%, as well as at the fully occupied B-site and sulfur at the fully occupied X-site (x, x, x) with $x = 0.2574$ close to the value 0.25 for the ideal spinel structure [8].

Only very limited information is available with respect to the magnetic properties of semiconducting FeIn_2S_4 (mineral name indite). Magnetic susceptibility and Mössbauer spectroscopic measurements between 77 K and room temperature revealed a Curie–Weiss behaviour with predominantly antiferromagnetic exchange interactions as indicated by a negative Curie–Weiss temperature of $\theta = -122$ K [9, 10]. Furthermore, a detailed structural study on single crystalline samples has been performed [12]. This cubic spinel compound exhibits an almost complete cation inversion with Fe^{2+} located at the octahedral sites only and In^{3+} at both tetrahedral and octahedral sites [10].

In the search for new materials revealing magnetic and semiconducting properties, a new compound has been synthesized by incorporating Fe into semiconducting In_2S_3 with a nominal composition of $\text{Fe}_{0.5}\text{In}_{1.5}\text{S}_3$. To the best of our knowledge, we are not aware of any report in the literature concerning mixed compounds of the series $\text{In}_2\text{S}_3\text{:FeIn}_2\text{S}_4$.

2. Experimental details

The samples were synthesized by a solid state reaction of the stoichiometric ratios of the pure elements (purity 5N) according to $\text{Fe}_{0.5}\text{In}_{1.5}\text{S}_3$ in sealed quartz ampoules under vacuum (10^{-4} mm of mercury). Sealed quartz ampoules filled with carefully stirred sample material were heated at a rate of 1.5 K min^{-1} up to the melting point of $T_m = 1183$ K, where the temperature was kept constant for 4 h. After slowly cooling the melt to room temperature the products were subsequently annealed for 4 weeks at 550°C before slowly cooling down again to room temperature. The actual molar composition was determined by EDX to be 56% S, 11% Fe and 32% In, respectively, indicating some deviations from the nominal stoichiometry.

The powdered polycrystalline samples were characterized by conventional x-ray powder diffraction at room temperature using Cu $K\alpha_1$ radiation. The data were analysed by standard Rietveld refinement employing the FULLPROF program [13]. Most importantly, the x-ray diffraction pattern showed single phase material. Within experimental accuracy, a satisfying refinement (with residuals of $R_{\text{Bragg}} = 6.5\%$) of the diffraction pattern could be achieved by adopting the spinel structure with cubic symmetry in space group $Fd\bar{3}m$ and a lattice constant of $a = 10.690(3)$ Å, where the occupancies have been restricted to the nominal stoichiometry $\text{Fe}_{0.5}\text{In}_{1.5}\text{S}_3$ and a statistical distribution of Fe and In ions was assumed. Then, both Fe and In ions occupy the A- and B-site, respectively, whereas sulfur occupies the X-site with the only positional parameter $x = 0.2576$. Varying the site occupation factors without stoichiometry constraints revealed some Fe deficiency in agreement with the EDX measurements. However, the quality of the fit could not be improved significantly. As will be explained below, neutron diffraction is much better suited to explore the cation distribution in detail.

Magnetic measurements were performed with a SQUID magnetometer for temperatures $1.8 \text{ K} < T < 400 \text{ K}$ and external magnetic fields $B_{\text{ex}} < 50 \text{ kOe}$.

Temperature-dependent ($1.6 \text{ K} < T < 280 \text{ K}$) neutron powder diffraction studies were performed on the fine-resolution diffractometer E9 at the BERII reactor of the Hahn-Meitner-Institut, Berlin [14, 15]. An incident neutron wavelength of $\lambda = 1.7976$ Å was selected by a Ge (511) monochromator. The multidetector array of the instrument covered an angular range of 155° with an angular step width of 0.078° .

3. Results and discussion

At elevated temperatures ($T > 20 \text{ K}$), the magnetic susceptibility of $\text{Fe}_{0.76}\text{In}_{2.17}\text{S}_4$ follows a Curie–Weiss law with a Curie–Weiss temperature of $\theta_{\text{CW}} = -50 \text{ K}$, thus indicating predominantly antiferromagnetic exchange interactions, and an effective paramagnetic moment of $\mu_{\text{para}}^{\text{eff}} = 4.6 \mu_{\text{B}}/\text{Fe}$. This is about 7% below the value expected for the high spin configuration ($S = 2$) of Fe^{2+} , which might be attributed to covalence effects. The temperature-dependent susceptibility of $\text{Fe}_{0.76}\text{In}_{2.17}\text{S}_4$ below $T < 15 \text{ K}$ is shown in figure 1 for various applied fields. For an external field of 100 Oe, the susceptibility shows a sharp cusp at 5 K with a clear splitting of the field-cooled (FC) and zero-field-cooled (ZFC) branch. Such a behaviour signals the onset of irreversibility in spin glass systems and is thus identified as the freezing temperature T_{F} . Upon increasing magnetic fields, the cusp becomes suppressed and the FC–ZFC splitting is shifted towards lower temperatures. It is interesting to note that the field dependence of the splitting just follows the ZFC branch in (virtual) zero field. A similar though less pronounced behaviour has recently been observed in aluminium spinels [16].

The real part of the ac-susceptibility in a driving field of 2 Oe is shown in figure 2 for various frequencies. A distinct shift of the cusp to higher temperatures upon increasing frequencies is observed. The initial frequency shift of T_{F} is $\delta T_{\text{F}} = \Delta T_{\text{F}} / (T_{\text{F}} \Delta \log_{10} \omega) = 0.035$, which is a typical value for metallic spin glasses like CuMn. Within the present frequency regime, the relaxation process can be described as a thermally activated behaviour with an attempt frequency of $\nu_0 \approx 10^{34} \text{ Hz}$ and an energy barrier of $E/k_{\text{B}} \approx 176 \text{ K}$, with k_{B} being the Boltzmann constant. Such an unphysical high value of ν_0 is a signature of the cooperative character of the freezing process which is typical for spin glass systems. In sum, the magnetic susceptibility of $\text{Fe}_{0.76}\text{In}_{2.17}\text{S}_4$ shows the typical signatures of a canonical low-temperature spin glass state.

High-resolution neutron powder diffraction experiments were performed for temperatures in between 1.6 and 280 K. In agreement with the x-ray diffraction data, all Bragg reflections of $\text{Fe}_{0.76}\text{In}_{2.17}\text{S}_4$ can be indexed by adopting the cubic spinel structure with space group $Fd\bar{3}m$.

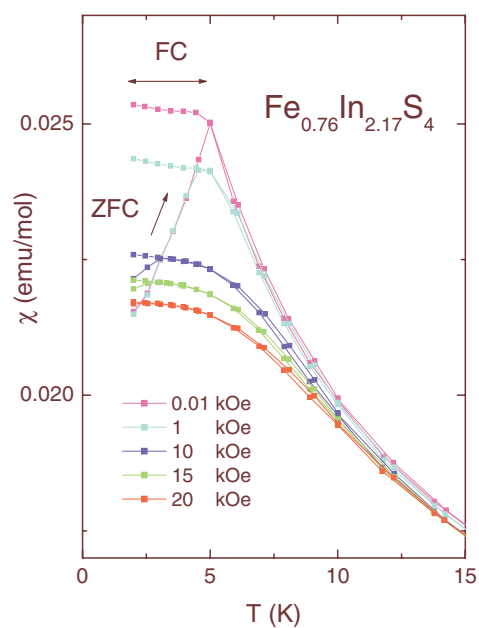


Figure 1. Temperature dependence of the dc-magnetic susceptibility of $\text{Fe}_{0.76}\text{In}_{2.17}\text{S}_4$ for various fields with a clear splitting of the field-cooled (FC) and zero-field-cooled (ZFC) branch, respectively. (Conversion factors to SI units: $1 \text{ emu mol}^{-1} = 10^{-3} \text{ A m}^2 \text{ mol}^{-1}$; $1 \text{ Oe} = 10^3/4\pi \text{ A m}^{-1}$).

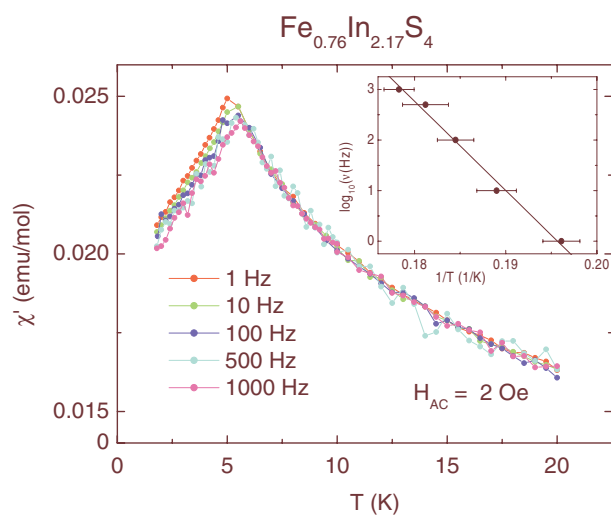


Figure 2. Frequency dependence of the real part of the ac-magnetic susceptibility of $\text{Fe}_{0.76}\text{In}_{2.17}\text{S}_4$ in a driving field of 2 Oe. The inset shows the logarithm of the frequency as a function of the inverse temperature of the cusp of the magnetic susceptibility. The straight line is a linear fit corresponding to a simple activated relaxational behaviour.

Within the given temperature range all diffraction patterns are very similar, indicating only very moderate structural changes. As an example, the diffraction pattern of $\text{Fe}_{0.76}\text{In}_{2.17}\text{S}_4$ at $T = 1.6 \text{ K}$ is shown in the main frame of figure 3. The refined parameters include background,

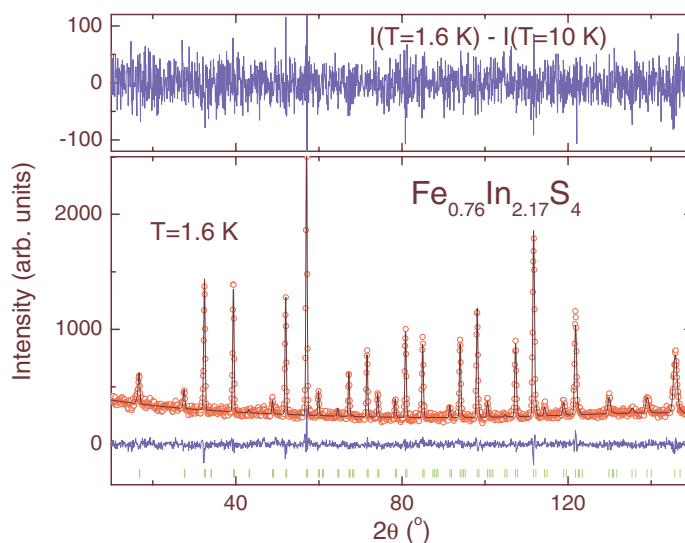


Figure 3. Lower main part: neutron powder diffraction pattern of $\text{Fe}_{0.76}\text{In}_{2.17}\text{S}_4$ at $T = 1.6$ K. Shown are the experimentally observed (open circles) and the refined calculated (full line) intensities. The difference is shown by the bottom line, and peak positions are indicated by the vertical bars. Upper part: difference of the diffraction intensities at $T = 10$ K (well above T_F) from $T = 1.6$ K (well below T_F) in order to evidence the absence of any significant magnetic scattering.

instrumental parameters (zero point shift and resolution parameters), lattice constant a , oxygen positional parameter x , site occupancies and isotropic temperature factors, respectively. No additional magnetic intensities could be detected at low temperatures, in agreement with a spin glass state. This is evidenced in the smaller upper panel of figure 3. Neither magnetic Bragg peaks, nor significant broad modulations of the intensity due to short range magnetic order, can be detected. Most likely, the Fe concentration is too small so that short range magnetic correlations are not reflected in appreciable magnetic scattering intensities.

Since a highly defective spinel structure is expected for $\text{Fe}_{0.76}\text{In}_{2.17}\text{S}_4$, an initial structural refinement was performed putting a single arbitrary ion on all three different crystallographic sites in order to determine the ratio of the scattering lengths. The successful refinement results in scattering length ratios of $b_{\text{coh}}(\text{A}):b_{\text{coh}}(\text{X}) = 0.306$ and $b_{\text{coh}}(\text{B}):b_{\text{coh}}(\text{X}) = 0.878$. As mentioned above, pure In_2S_3 may be written as $\text{In}_{0.67}\text{In}_2\text{S}_4$ with one third of vacancies at the A-site, and FeIn_2S_4 exhibits a spinel structure with almost complete cation inversion [12]. Considering the different electronic configurations we note In^{3+} , Fe^{2+} and S^{2-} , respectively [10]. In order to consistently account for the actual stoichiometry as determined by EDX, charge neutrality demands a composition of $\text{Fe}_{0.76}\text{In}_{2.17}\text{S}_4$. The present compound thus exhibits In excess and Fe deficiency. The molar composition together with the scattering length ratios of the different crystallographic sites then leads to a set of linear equations that determine the cation distribution among the A- and B-sites, respectively [11]. As documented by the site occupation factors in table 1, an almost complete cation inversion parameter of 0.94(2) as the percentage of Fe ions at the octahedral B-site has been determined, in excellent agreement with structural data from single crystal x-ray diffraction experiments on FeIn_2S_4 [12]. The present spinel compound may thus be described as $(\text{Fe}_{0.04}\text{In}_{0.89}\square_{0.07})^{\text{A}}(\text{Fe}_{0.72}\text{In}_{1.28})^{\text{B}}\text{S}_4$ with 7% vacancies at the tetrahedral A-site. Within the given experimental accuracy, the refinement resulted in a constant oxygen position at (x, x, x) with $x = 0.2591(1)$, close to 0.25 of the

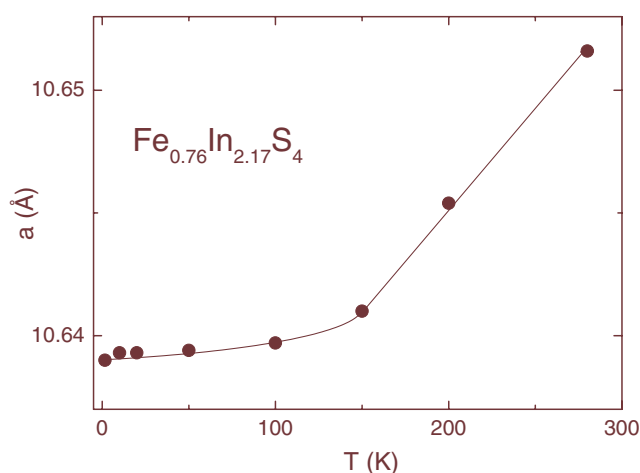


Figure 4. Temperature-dependent lattice parameter of $\text{Fe}_{0.76}\text{In}_{2.17}\text{S}_4$ as deduced from the Rietveld refinements of the neutron powder diffraction data. Errors are within the symbol size.

Table 1. Structural parameters of $\text{Fe}_{0.76}\text{In}_{2.17}\text{S}_4$ as resulting from the Rietveld refinements within space group $Fd\bar{3}m$. Listed are the lattice parameter a , site occupation factors (SOFs) with respect to the fully occupied sulfur position, and the residuals R_{Bragg} .

T (K)	a (Å)	SOF In(8a)	SOF Fe(8a)	SOF In(16d)	SOF Fe(16d)	R_{Bragg}
1.6	10.6390(1)	0.913(10)	0.017(10)	0.629(10)	0.372(10)	0.060
10	10.6393(1)	0.907(10)	0.023(10)	0.632(10)	0.369(10)	0.056
20	10.6393(2)	0.869(11)	0.061(11)	0.651(11)	0.350(11)	0.060
50	10.6394(1)	0.896(10)	0.034(10)	0.637(10)	0.363(10)	0.049
100	10.6397(1)	0.881(11)	0.049(11)	0.645(11)	0.356(11)	0.063
150	10.6410(2)	0.875(13)	0.055(13)	0.648(13)	0.353(13)	0.064
200	10.6454(2)	0.887(11)	0.043(11)	0.642(11)	0.359(11)	0.070
280	10.6516(2)	0.891(12)	0.039(12)	0.640(12)	0.361(12)	0.081

ideal spinel structure. The structural parameters of $\text{Fe}_{0.76}\text{In}_{2.17}\text{S}_4$ as resulting from the final Rietveld refinements are summarized in table 1.

The temperature dependence of the lattice parameter is shown in figure 4. It remains virtually constant up to 100 K before a moderate thermal expansion occurs. The overall change of the lattice parameter from 1.6 to 280 K is 0.1% only. Very similar thermal behaviours are found in other sulfur spinels, namely in FeSc_2S_4 , MnSc_2S_4 , Co_3S_4 and CuCo_2S_4 which are currently being studied.

An evaluation of the reliability of the refinement may be performed as follows. First, it is noted that the spinel structure type is an archetypical example of a cubic close-packed structure that is usually considered as an fcc anion lattice exhibiting tetrahedral and octahedral interstitial sites, respectively. This justifies the assumption of a fully occupied X-site as it is usually employed for spinel compounds in general. Considering the accuracy of the cation distribution, it is noted that the standard deviation of the EDX measurements are 0.36% and 0.21% for Fe and In, respectively. Moreover, the standard deviation of the site occupancy (see table 1) results in an uncertainty of the average scattering length. Both factors finally lead to an error of 2% in the actual cation distribution; i.e. $\text{Fe}_{0.04 \pm 0.02}\text{In}_{0.89 \pm 0.02}\square_{0.07 \pm 0.02}$ for the A-site occupancy. According to this error consideration the occupancy of Fe at the A-site is significant. The reason is that the coherent neutron scattering length of Fe (9.45 fm)

is much larger than those of In (4.065 fm) and S (2.847 fm), respectively. The values of the neutron scattering lengths as compared to the corresponding x-ray form factors are also the reason why neutron diffraction is much better suited for a detailed exploration of the cation distribution than are x-ray diffraction measurements. As mentioned above, an initial refinement of the x-ray diffraction data was performed with constraints of the occupancies according to the nominal stoichiometry ($\text{Fe}_{0.5}\text{In}_{1.5}\text{S}_4$) and a statistical distribution of both kinds of cations among the A- and B-sites, respectively. Employing x-ray form factors, this results in a ratio of $f_{\text{A}}:f_{\text{B}}:f_{\text{X}} = 1:1.197:0.61$. The corresponding x-ray form factor ratios on the basis of the finally determined structure of $\text{Fe}_{0.76}\text{In}_{2.17}\text{S}_4$ result in very similar ratios of $f_{\text{A}}:f_{\text{B}}:f_{\text{X}} = 1:1.287:0.69$. By contrast, employing coherent neutron scattering lengths for the two structural models results in ratios of either $b_{\text{A}}:b_{\text{B}}:b_{\text{X}} = 1:0.878:0.306$ or, on the other hand, $b_{\text{A}}:b_{\text{B}}:b_{\text{X}} = 1:0.416:0.416$, respectively.

The crystal structure also provides the basis for a natural explanation of the spin glass ground state. Frustration characterizes the inability of a system to satisfy all pairwise interactions and to establish a unique long-range ordered ground state, despite strong interactions. In the present case of $\text{Fe}_{0.76}\text{In}_{2.17}\text{S}_4$, the Curie–Weiss temperature of $\theta_{\text{CW}} = -50$ K reflects the energy scale of the effective antiferromagnetic exchange interactions. However, the system remains paramagnetic down to $T_{\text{F}} = 5$ K, which is an order of magnitude lower than θ_{CW} . Such a behaviour is a typical signature of dominant frustration effects inhibiting the formation of long-range magnetic order. Instead, a highly degenerate ground state is formed. Frustration combined with disorder provides the key concept to understand the spin-glass state in disordered magnets [17]. Already in 1956 Anderson [18] pointed out that the octahedral B-sites of the spinel structure form a frustrated lattice in which it is possible to achieve perfect short-range order while maintaining a finite entropy. In fact, the B-site sublattice can be directly mapped onto the pyrochlore lattice, and it forms a network of corner-sharing tetrahedra. Due to the constituent triangles, each tetrahedron is geometrically highly frustrated for nearest neighbour antiferromagnetic exchange interactions. The structural refinements of $\text{Fe}_{0.76}\text{In}_{2.17}\text{S}_4$ show that the B-sites are statistically occupied to 37% by magnetic Fe^{2+} ions, which in turn provides a high degree of atomic disorder. The presence of strong geometric frustration combined with a high degree of disorder then naturally leads to the formation of a spin glass ground state.

4. Conclusion

Summarizing, we have newly synthesized an iron-doped derivative of semiconducting In_2S_3 . The strongly inverse cubic spinel type structure has been found with both the tetrahedral A-sites and the octahedral B-site partly occupied by Fe and In, respectively. Magnetic measurements reveal a canonical spin glass state at low temperatures. This behaviour can be naturally explained on the basis of the actual stoichiometry and the crystal structure. For nearest neighbour antiferromagnetic superexchange interactions, the spinel structure exhibits strong geometric frustration of both the A- and B-site sublattice, respectively. In combination with the considerable atomic disorder, this provides the necessary conditions for the occurrence of a spin glass state.

Acknowledgments

This work was supported by the BMBF under Contract No 13N6917-A/Elektronische Korrelationen und Magnetismus (EKM) and by the Deutsche Forschungsgemeinschaft (DFG) via SFB484/Augsburg. We thank D Vieweg for magnetic measurements and Dr M Klemm for the EDX analysis.

References

- [1] Ohno H, Munekata H, Penney T, von Molnar S and Chang L L 1992 *Phys. Rev. Lett.* **68** 2668
- [2] Ohno H, Shen A, Matsukura F, Oiwa A, Endo A, Katsumoto S and Iye Y 1996 *Appl. Phys. Lett.* **69** 363
- [3] Sirimanne P M, Yasaki Y, Sonoyama N and Sakata T 2002 *Mater. Chem. Phys.* **78** 234
- [4] Barreua N, Bernède J C, Marsillac S and Mokrani A 2002 *J. Cryst. Growth* **235** 439
- [5] Diehl R and Nitsche R 1975 *J. Cryst. Growth* **28** 306
- [6] Steigmann G A, Sutherland H H and Goodyear J 1965 *Acta Crystallogr.* **19** 967
- [7] Diehl R, Nitsche R and Carpentier C-D 1973 *J. Appl. Crystallogr.* **6** 497
- [8] Likforman A, Guittard M, Tomas A and Flahaut J 1980 *J. Solid State Chem.* **34** 353
- [9] Eibschütz M, Hermon E and Shtrikman S 1967 *Solid State Commun.* **5** 529
- [10] Yagnik C M and Mathur H B 1967 *Solid State Commun.* **5** 841
- [11] Battle X, Obradors X, Rodriguez-Carvajal J, Pernet M, Cabanas M V and Vallet M 1991 *J. Appl. Phys.* **70** 1614
- [12] Hill R J, Craig J R and Gibbs G V 1978 *J. Phys. Chem. Solids* **39** 1105
- [13] Rodriguez-Carvajal J 1993 *Physica B* **192** 55
- [14] Többs D M, Stüßer N, Knorr K, Mayer H M and Lampert G 2001 *Mater. Sci. Forum* **378–381** 288
- [15] Többs D M and Tovar M 2002 *Appl. Phys. A* **74** (Suppl.) S136
- [16] Tristan N *et al* 2005 *Phys. Rev. B* submitted
- [17] Binder K and Young A P 1986 *Rev. Mod. Phys.* **58** 801
- [18] Anderson P W 1956 *Phys. Rev.* **102** 1008